Investigation of the defect complexes in highly Mg-doped LiNbO$_3$ crystals by ^{93}Nb NMR method

A.V.Yatsenko, S.V.Yevdokimov, D.Yu.Sugak$^{*, **}$, I.M.Solskii**

Taurida National V.Vernadskii University, 4 Vernadskii Ave.,
95007 Simferopol, Ukraine
*Lviv Polytechnic National University, 12 Bandera Str.,
79000 Lviv, Ukraine
**Scientific Research Company "Carat", 202 Stryjska Str.,
79031 Lviv, Ukraine

Angular dependence of the line width of the ^{93}Nb NMR spectrum central transition for LiNbO$_3$ crystal with congruent composition and for the samples with high Mg concentration was experimentally investigated. Having the experimental results compared with the results obtained by computer simulation, it has been concluded that the most probable type of defects in magnesium doped LiNbO$_3$ crystals are (4Mg$_{Li}^{2+}$ + 4V$_{Li}$) defect complexes when four Li vacancies and three Mg$_{Li}^{2+}$ ions being localized in the seven nearest positions to the central Mg$_{Li}^{2+}$ ion.

Экспериментально исследована угловая зависимость ширины линии центрального перехода спектра ЯМР ^{93}Nb в кристалле LiNbO$_3$ конгруэнтного состава и образцах с высокой концентрацией Mg. На основании сравнения экспериментальных результатов с результатами компьютерного моделирования делается вывод, что основным типом дефектов в кристаллах LiNbO$_3$ с примесью магния являются дефектные комплексы (4Mg$_{Li}^{2+}$ + 4V$_{Li}$), причем четыре вакансии ионов Li и три иона Mg$_{Li}^{2+}$ локализованы в семи ближайших от центрального иона Mg$_{Li}^{2+}$ позициях ионов Li.

***Дослідження дефектних комплексів у сильно легованих Mg кристалах LiNbO$_3$ методом ЯМР ^{93}Nb**. О.В.Яценко, С.В.Євдокимов, Д.Ю.Сугак, І.М.Сольський*. Експериментально досліджено кутову залежність ширини лінії центрального переходу спектра ЯМР ^{93}Nb у кристалі LiNbO$_3$ конгруентного складу та зразках з високою концентрацією Mg. На підставі порівняння експериментальних результатів з результатами комп'ютерного моделювання робиться висновок, що основним типом дефектів у кристалах LiNbO$_3$ з домішкою магнію є дефектні комплекси (4Mg$_{Li}^{2+}$ + 4V$_{Li}$), причому чотири вакансії іонів Li та три іони Mg$_{Li}^{2+}$ локалізовані у семи найближчих від центрального іона Mg$_{Li}^{2+}$ позиціях іонів Li.

1. Introduction

Lithium niobate (LN) crystals have found their very wide application in modern nonlinear optics, optoelectronics and acoustoelectronics [1]. It is known that Mg- or Zn-doped LN crystals with impurity concentration exceeding some threshold value, become insensitive to the light fluxes [2], and this has given rise to an intensive study of their physical properties.

The Mg-doped LN crystals are usually grown by the Czochralski technique from the stoichiometric mixture, with necessary

quantity of MgO [3] being added. While extensive researches are dealing with the growth and properties of $LiNbO_3$:MgO crystals, there are still discussions about the mechanisms for incorporation of Mg^{2+} ions into the lithium niobate structure, and for compensating their electrical charge [4]. However, most researchers agree with the fact that when the Mg^{2+} ions concentration equals the threshold one, they totally prevent the Nb ions occupying the Li positions (antisite Nb_{Li} ions) [5–9].

Further important information on the defect centers in the lithium niobate crystals, including those occurring within the processes of their doping with MgO, can be obtained by NMR method.

For example, in [10], the structure of defect centers in Mg doped LN crystals has been investigated by applying the ^7Li NMR and studying a series of $LiNbO_3$ crystals with various Mg concentrations. Based on the concentration dependence of the NMR spectrum linewidth, a conclusion has been made that there is a high probability of formation of the defect complexes, each of which includes Mg_{Li} ion and Li vacancy (V_{Li}) located on the shortest distance between them. The analysis carried out in [10] for occupation of the cations' structural positions in the Mg-doped LN crystals has shown that the chemical formula of the LN crystal with threshold Mg concentration can be written as $[Li_{1-2x}Mg_x\square x]NbO_3$, where $x\cong 0.05$, and ($\square$) denotes the structural vacancy.

It is also known that increasing of Mg concentration in the LN crystals is accompanied by the central transition line broadening in the ^{93}Nb NMR spectrum [11, 12]. Thus, research and analysis of the NMR spectra of ^{93}Nb nuclei shall be an effective tool in studying the defect structure of the LN crystals with various Mg concentration. It has been shown earlier [13], that the comparing the results of simulation of the ^{93}Nb NMR spectra in the congruent LN crystals with the experimental ones makes possible to obtain the most probable realization of the defect crystal structure.

The purpose of this work was to investigate the defect structure of the LN crystals, grown from a congruent melt with addition of high quantity MgO, by carrying out experimental investigation of the NMR spectra and their comparison with the parameters of the NMR spectra, simulated taking into account the calculations of electric field gradient (EFG) at ^{93}Nb nuclei according to different kinds of the defect crystal structure.
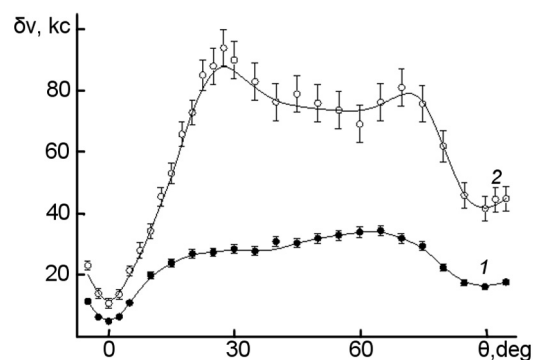

Fig. 1. Angular dependences of the ^{93}Nb NMR spectrum central line width (δv) in the nominally pure congruent LN crystal (*1*) and in the crystal with 5.0 mol. % MgO content (*2*). The dependence (*2*) is spline-approximated within the experiment error. For the nominally pure sample the results of computer simulations of the spectrum (solid line) against the model of lithium vacancies [13] are given.

2. Experimental investigation of ^{93}Nb NMR in $LiNbO_3$ crystals

To investigate parameters of the central transition line of the ^{93}Nb NMR spectrum we used the samples of nominally pure congruent LN single crystals and two MgO-doped LN single crystals which have been grown by the Czochralski method at the SRC "Carat" using the procedure described in [3, 14]. MgO content in these crystals has been determined by chemical and photochemical analysis methods and it was equal to (5.0±0.5) and (7.0±0.5) mol. %. The excess above the threshold concentration of Mg ions has been confirmed by investigating the EPR spectra of the uncontrolled impurity of Fe ions in the crystals obtained [3].

The LN crystals have clearly marked piezoelectric properties, which makes it significantly difficult to investigate them by the NMR pulse methods [15]. Therefore, the experiments have been carried out using a continuous-wave NMR spectrometer with an autodyne detector under magnetic field of 1.4 T using a technique of multiple accumulation and digital filtration of spectra [16].

It has been shown earlier that in comparison of the results of simulation of the ^{93}Nb NMR spectra in congruent LN crystals with the experimental ones, it is more convenient to analyze the dependence of the ^{93}Nb NMR spectrum central transition linewidth on angle θ between the crystal three-fold symmetry axis **c** and the direction of external magnetic field **B**$_0$.

Fig. 1 illustrates the dependence of the ^{93}Nb NMR spectrum central line width (δv) on the angle θ between the crystal's 3-fold symmetry axis **c** and the direction of external magnetic field $\mathbf{B}_0$ for a nominally pure sample, and for the crystal containing 5.0 mol. % MgO. It should be noted that the dependence $\delta v(\theta)$ for this pure LN sample within the error limits matches the known results obtained in investigating other congruent LN sample under the same experiment conditions [13]. This figure also shows the dependence $\delta v(\theta)$ which has been earlier obtained by simulation of the ^{93}Nb NMR spectra in a nominally pure congruent LN crystal [13]. Experimentally obtained data for the sample, containing 7.0 mol. % MgO will be given in the next part of the paper.

3. Simulation of ^{93}Nb NMR spectrum

In our work we have presumed that the magnesium ions which are incorporate in LiNbO$_3$ structure can occupy only Li positions, so the structural formula of the LN crystal with a high (overthreshold) Mg concentration takes the form:

$$[Li_{1-2x}Mg_x\square_x]NbO_3,$$
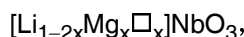
where $x \geq 0.05$, and the symbol ($\square$) denotes the structural vacancy. Fig. 2 shows the nearest cationic surrounding of Mg_{Li}^{2+} ion. In terms of observing the crystal lattice electroneutrality principle it is necessary to presuppose that the lithium vacancy V_{Li} compensating the impurity's excess charge which is localized in one of the eight positions of Li$^+$ ions as highlighted in Fig. 2.

The best method for simulation of the NMR spectra of a quadrupolar nuclei in single crystals is based on calculating the sets of the EFG tensor realizations at the nuclei under investigation [13]. In our case the volume concentration of defects is very high, and average distance between the defects is only 0.8 nm. A strong cross-impact of the defects makes it impossible to calculate the EFG in such defective structure using *ab initio* approaches [17].

To simulate the ^{93}Nb NMR spectra we used the algorithm proposed earlier [13], which includes the random location of the defects or defect complexes in the crystal structure and further calculation of the sets of the possible EFG tensor realization according to the modified point- multipole approach. As a result, more than 4000 realiza-
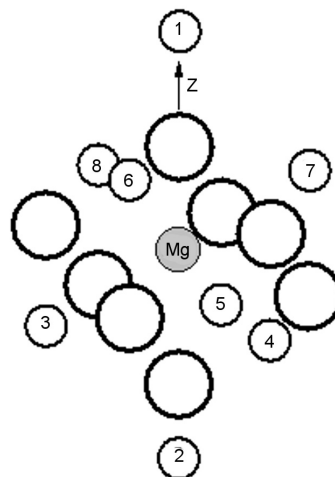

Fig. 2. The nearest cationic surrounding of Mg_{Li}^{2+} ion. Li$^+$ ions are shown by small numbered circles; Nb ions are shown by the large ones. Arrow indicates the direction of the crystal polar axis.

tions of the EFG tensor at ^{93}Nb nuclei were obtained and took into consideration for the simulation of the NMR line shapes. For simulation of the action of local distortions of the crystal structure, caused by the defects, the additional dispersion of the principal axes orientation of the EFG tensor and dispersion of its main value were introduced for the final calculations.

To analyze the degree to which the defectiveness models under consideration conform to the experimental results the following criterion has been used — the relative *rms* deviation σ_v of the estimated value of the line width (δv_c) from the experimental value (δv_e):

$$\sigma_v = \left\{ \frac{1}{n}\sum_{i=1}^{n} \left[\frac{(\delta v_c)_i - (\delta v_e)_i}{\delta v_e} \right]^2 \right\}^{1/2},$$

where n is the number of points of the experimental angular dependence $\delta v(\theta)$) within the range $12.5° \leq \theta \leq 90°$.

At the first stage of simulations we considered the simplest possible realizations of the defect structure in LN:Mg with the threshold Mg content which are given in the Table 1. It was concluded that simulation according to the model "m6" in the best manner corresponds to the experimental data in the case of LN doped by 5.0 mol.% MgO and respective σ_v value is equal to 9.5 %. Nevertheless simulation of the ^{93}Nb

Table 1. The simplest possible realizations of $LiNbO_3$:Mg defect structure

Realizations of the defect structure	Model
Independent localization of Mg_{Li}^{2+} and V_{Li}	m1
Pairs (Mg_{Li}^{2+} + V_{Li}), where V_{Li} is localized in 1-st position of Li ions (Fig. 2)	m2
Pairs (Mg_{Li}^{2+} + V_{Li}), where V_{Li} is localized in 2-nd position of Li ions (Fig. 2)	m3
Pairs (Mg_{Li}^{2+} + V_{Li}), where V_{Li} is localized equally probable in the positions (3), (4), (5)	m4
Pairs (Mg_{Li}^{2+} + V_{Li}), where V_{Li} is localized equally probable in the positions (6), (7), (8)	m5
Pairs (Mg_{Li}^{2+} + V_{Li}), where V_{Li} is localized equally probable in the positions (3)÷(8)	m6

Table 2. More complicate realizations of the defect structure

V_{Li} are localized in the next positions: *	Mg_{Li} are localized in the next positions: *	Model	Smallest σ_v, %	
			5.0 % MgO	7.0 % MgO
(2), (3), (4), (5)	(6), (7), (8)	c1	9.5	14.3
(1), (3), (4), (5)	(6), (7), (8)	c2	9.3	13.4
(1), (6), (7), (8)	(3), (4), (5)	c3	9.6	13.5
(2), (6), (7), (8)	(3), (4), (5)	c4	10.5	15.1
two from (3), (4), (5) one from (6), (7), (8) and in (1)	two from (6), (7), (8) one from (3), (4), (5)	c5	11	18.0
two from (3), (4), (5) one from (6), (7), (8) and in (2)	two from (6), (7), (8) one from (3), (4), (5)	c6	10.3	17.0

* Numeration of positions — according to Fig. 2.

NMR spectra for crystal which contains 7.0 mol. % MgO according to the models, which are listed in Table 1, demonstrates the largest differences between experimental and simulated results — the best obtained σ_v value in these cases was equal to 16.5 %.

And so we take into consideration the more complicate defect complexes, which contains of $4Mg_{Li}$ ions and $4V_{Li}$ at the shortest distances. Some realizations of such complicate defect complexes, which we analyzed, are presented in Table 2. The lowest values of σ_v which were obtained by comparing the experimental and simulated data are listed in Table 2 too.

In spite of all configurations of the defect complexes (c1–c6) it provides a good correspondence of the experimental and simulated data for the sample which contains 5 % MgO, only complexes marked as (c1–c4) give the minimal σ_v values for the sample with 7 % MgO. The best results were obtained when the [93]Nb NMR spectra were simulated according to the models

"c2" and "c3". The angular dependences of the [93]Nb NMR linewidth for both Mg-contained samples, simulated according to the model "c2" are shown in Fig. 3 and Fig. 4.

4. Discussion

It is marked above already, that the average distance between the defects in highly Mg doped LN crystals is relatively small, so even in the assumption of random distribution of Mg_{Li} and V_{Li} in the crystal lattice the probability of occupying two neighbor Li position by Mg_{Li} and V_{Li} is very high. It leads to appearance of different kinds of (Mg_{Li}^{2+} + V_{Li}) pairs which are listed in Table 1. Nevertheless the investigations of the defect structure of undoped congruent LN crystals show that the preliminary defects in this crystal are the defect complexes (Nb_{Li}^{5+} + $4V_{Li}$) when three V_{Li} locates at the nearest neighbors Li sites, forming a vacancy triangle under Nb_{Li} site, and fourth V_{Li} locates relatively far away [13, 18] or in one of the Li sites in upper Li triangle [19].
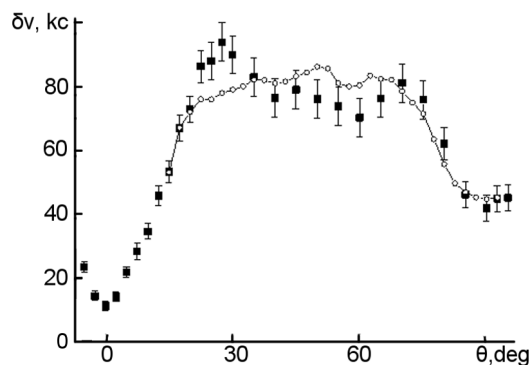
Fig. 3. Angular dependences of the ^{93}Nb NMR spectrum central linewidth (δv) in the crystal with 5.0 mol. % **MgO** content. Squares indicates the experimental data, open circles indicates the best results of computer simulations according to the model "c2".
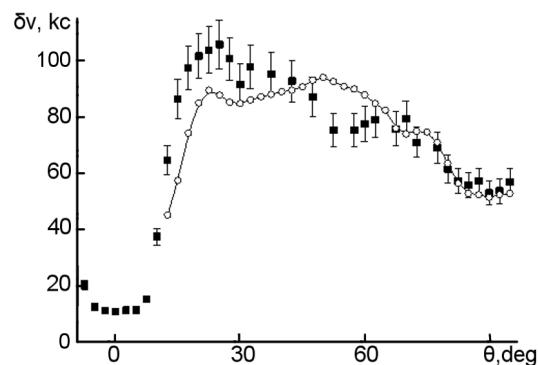
It is concluded, that the latest configuration [19] is energetically favorable. So it is very possible that forming the ($4Mg_{Li}^{2+}$ + $4V_{Li}$) defect complexes in highly **Mg** doped **LN** crystal is energetically favorable too.

6. Conclusions

It can be concluded, that the most possible type of defects in **LN** crystal with the threshold and highest **Mg** content are the defect complexes ($4Mg_{Li}^{2+}$ + $4V_{Li}$) in configurations presented by the models "c2" or "c3" in Table 2. The most likely causes of partial discrepancy between the simulated and experimental ^{93}Nb spectra can be first of all neglecting the real local distortions of the crystal structure of the defect complexes and its nearest surrounding in the process of simulations of the NMR spectra.

It should be noted that there are another (not considered above) models of the defect structure of **LiNbO$_3$:Mg** crystals. First of all it is possible, that at high concentrations (over the threshold value) **Mg** ions partially occupied not only **Li** sites but **Nb** sites too [9]. In [20] dealing with the investigation of the properties of **LN** crystals with **Zn** impurity, it has been supposed that **Zn^{2+}** ions do not occupy the position of **Li** ions, but are displaced into an unoccupied octahedron. Simulations of the ^{93}Nb NMR spectra according these models are in progress now and will be a subject of the next paper.

References

1. L.Arizmendi, *Phys. Stat. Sol. (a)*, **201**, 253 (2004).

Fig. 4. Angular dependences of the ^{93}Nb NMR spectrum central linewidth (δv) in the crystal with 7.0 mol. % **MgO** content. Squares indicates the experimental data, open circles indicates the best results of computer simulations according to the model "c2".

2. U.Schlarb, K.Betzler, *Phys. Rev. B*, **50**, 751 (1994).
3. D.Yu.Sugak, A.O.Matkovskii, I.M.Solskii et al., *Cryst. Res. Technol.*, **32**, 805 (1997).
4. T.Volk, M.Wohlecke, Lithium Niobate. Defects, Photorefraction and Ferroelectric Switching, Berlin, Springer (2008).
5. K.Polgar, L.Kovacs, I.Foldvari et al., *Solid State. Commun.*, **59**, 375 (1986).
6. L.Palfalvi, J.Hebling, G.Almasi et al., *J. Appl. Phys.*, **95**, 902 (2004).
7. F.Abidi, M.Aillerie, M.Fontana et al., *Appl. Phys. B*, **68**, 795 (1999).
8. R.Mouras, M.Fontana, P.Bourson et al., *J. Phys.:Condens. Matter.*, **12**, 5053 (2000).
9. K.Lengyel, L.Kovacs, A.Peter, *Appl. Phys. B*, **87**, 317 (2007).
10. A.V.Yatsenko, S.V.Yevdokimov, D.Yu.Sugak et al., *Acta Phys. Polonica A*, **117**, 166 (2010).
11. L.Hu, Y.Chang, C.Chang et al., *Modern Phys. Lett. B*, **5**, 789 (1991).
12. G.Malovichko, V.Grachev, O.Shirmer, *Appl. Phys. B*, **68**, 785 (1999).
13. A.V.Yatsenko, H.M.Maksimova, N.A.Sergeev, *Ukr. J. Phys.*, **44**, 1390 (1999).
14. I.M.Solskii, D.Yu.Sugak, V.M.Gaba, *Technologija i Konstruirovanie v Electronnoi Apparature*, **5**, 51 (2005).
15. C.Mignon, Y.Millot, P.Man, *C. R. Chimie*, **7**, 425 (2004).
16. A.V.Yatsenko, V.A.Kornienko, *Ukr. Zh. Fiz.*, **41**, 636 (1996).
17. M.G.Shelyapina, V.S.Kasperovich, B.F.Shchegolev et al., *Phys. Stat. Sol. B*, **225**, 171 (2001).
18. S.Kim, V.Gopalan, K.Kitamura et al., *J. Appl. Phys.*, **90**, 2949 (2001).
19. H.Xu, D.Lee, S.B.Sinnott et al., *J. Phys.:Condens. Matter.*, **22**, 135992 (2010).
20. G.Torchia, J.Tocho, F.Jaque, *J. Phys. Chem. Solids*, **63**, 555 (2002).